

RECEIVED: May 21, 2024

ACCEPTED: July 29, 2024

PUBLISHED: August 23, 2024

BBN catalysis by doubly charged particles

Evgeny Akhmedov^a and Maxim Pospelov^{b,c}

^aMax-Planck-Institut für Kernphysik,
Saupfercheckweg 1, 69117 Heidelberg, Germany

^bWilliam I. Fine Theoretical Physics Institute,
School of Physics and Astronomy, University of Minnesota,
Minneapolis, MN 55455, U.S.A.

^cSchool of Physics and Astronomy, University of Minnesota,
Minneapolis, MN 55455, U.S.A.

E-mail: akhmedov@mpi-hd.mpg.de, pospelov@umn.edu

ABSTRACT: We consider primordial nucleosynthesis in the presence of hypothetical quasi-stable doubly charged particles. Existence of X^{--} with macroscopic lifetimes will lead to the formation of its bound states with ^4He and other light elements, significantly facilitating the subsequent formation of lithium nuclei. From observational constraints on maximum allowable amount of lithium, that we update in this work, we derive strong constraints on the abundance and lifetime of X^{--} . In a likely cosmological freeze-out scenario with temperatures initially exceeding the mass of X^{--} , the BBN constrains the lifetime of these particles to be less than about 100 seconds. For parametrically long lifetimes, lithium abundance data constrain X^{--} abundance to be less than 10^{-9} relative to protons, regardless of whether these particles decay or remain stable. Stable particles could saturate the dark matter density only if their mass is comparable to or in excess of 10^{10} GeV, and most of X^{--} will be found in bound states with beryllium nuclei, so that chemically they would appear as abnormally heavy helium isotopes.

KEYWORDS: big bang nucleosynthesis, particle physics - cosmology connection, dark matter theory

ARXIV EPRINT: [2405.06019](https://arxiv.org/abs/2405.06019)

JCAP08(2024)028

Contents

1	Introduction	1
2	Observational constraints of primordial Li/Be/B	3
3	Properties of bound states and recombination rates	7
4	Catalyzed reactions	12
5	CBBN yields of Li/Be/B	15
6	Constraints from searches for heavy isotopes of H and He	17
7	Discussion and conclusions	20

1 Introduction

Metastable charged particles occur in many extensions of the Standard Model (SM) of particle physics. If the charge of such beyond-SM (BSM) particles is not small compared to the electron charge, they are guaranteed to be at or above the electroweak scale, given the capacity of modern experiments at the LHC as well as past experiments at LEP and the Tevatron. What sets charged particles in a completely different category from any BSM neutral metastable particle is the plethora of new phenomena that the charge implies. These additional signatures afford new experimental pathways for searches for such particles, see e.g. the review [1].

Chiefly among important experimental signatures for charged metastable particles X stands the presence of ionization tracks. For particles that interact solely due to electromagnetic interactions, the slow-down process is very inefficient, $|dE_X/dx| \sim |dE_\mu/dx|$, and given a large reservoir of kinetic energy, this results in long persistent ionizing tracks. The search for such tracks is performed both at ATLAS and the CMS experiments [2, 3], resulting in sensitivity to X at the level of a few hundred GeV (assuming standard electromagnetic or electroweak pair production mechanisms). The presence of charge also gives reasons to believe that “almost” stable particles can be accelerated at astrophysical sites and can be present as a rare component of cosmic rays (CR). This opens up the possibility to extend such searches much beyond the electroweak scale [1], modulo of course the assumption about the overall abundance of such particles.

Negatively charged massive particles X^- are of special interest. It is well known that they can form bound states with nuclei, thereby reducing the Coulomb barrier and facilitating nuclear reactions. Muon-catalyzed fusion reactions have been investigated over a number of years [4], and some exotic BSM possibilities for the catalysis were also discussed [5]. The two limiting factors that complicate any practical use of muon catalysis are the relatively short muon lifetime and formation of bound states with $Z \geq 2$ nuclei that “hide” μ^- from subsequent participation in nuclear fusion. Recently, it was argued that a heavy BSM

doubly-charged particle X^{--} would offer a huge advantage over X^- and would potentially be able to catalyze enough reactions to achieve positive energy balance, i.e. have energy release in excess of the energy needed for production or acquisition of such a particle [6]. Despite a rather futuristic nature of such investigations, it is important to have an example of a “useful” BSM particle, as this may give a new impetus to collider and CR searches of X^{--} . Incidentally, a recent ATLAS analysis [7, 8] showed some hints of the ionization tracks at the LHC with $|dE/dx|$ larger than that for muons, prompting the speculations that such tracks correspond to exotic X^{--} or X^{++} [9, 10].

One of the most important defining properties of a charged BSM particle is its lifetime. The LHC studies could potentially determine that the lifetime of X along the anomalous track is in excess of e.g. 10 ns. Cosmic ray searches on the other hand would be sensitive to particles with lifetimes $> \mathcal{O}(\text{years})$. This leaves many orders of magnitude in between, where only indirect studies are possible. The purpose of this work is to investigate the constraints on the lifetime and abundance of X^{--} imposed by cosmology, and specifically by the Big Bang Nucleosynthesis (BBN). It is well known that the presence of singly charged X^- with lifetimes in excess of $\mathcal{O}(10^3 \text{ s})$ in the early Universe leads to the catalysis of certain nuclear reactions and increased yield of such rare elements as ${}^6\text{Li}$ (the scenario known as CBBN) [11]. Observations of these elemental abundances, in turn, set strong constraints on the early Universe abundance of X^- , *irrespective* of subsequent fate of X^- (whether it decays or remains stable). Of course, if a particle decays, more constraints on energy injection during the BBN and cosmic microwave background (CMB) epochs would apply (see e.g. BBN review in [12] and references therein). The energy injection constraints are, however, quite model dependent. The BBN catalysis by X^{--} and consequent constraints on the abundance and lifetime of such a particle have not been studied thus far, and our goal is to fill this gap. We note that in addition to the motivations stated above, stable X^{--} particles that form bound states with helium and beryllium nuclei have been suggested as dark matter (DM) candidates in a number of publications [13, 14]. Our analysis on the abundance of X^{--} during the BBN would then provide a *lower limit* for the mass of such DM particles.

If the lifetimes of the doubly charged particles are comparable to or longer than the age of the Universe, such remnants could still be present, in particular, in the solar system, and on Earth. A doubly positively charged particle X^{++} would appear as an abnormally heavy helium, and in a certain mass range its abundance will be limited by the negative results of searches for anomalously heavy helium isotopes [15]. In addition, the BBN-generated yield of $(\text{Be}X^{--})$ bound states¹ will also be seen as abnormal helium, and will be present even if the evolution of the “ X -sector” is charge-asymmetric, so that X^{++} are not currently around. Moreover, the bound state of X^{--} with lithium isotopes will be chemically equivalent to hydrogen, and in a certain mass range will be subject to the very sensitive searches for anomalously heavy hydrogen performed long time ago [16, 17]. Determining the yields of $(\text{Be}X^{--})$ and $(\text{Li}X^{--})$ is another goal of our paper.

The existence of doubly-charged particles in BSM models is not guaranteed. Indeed, the SM itself does not contain elementary doubly charged states (as opposed to composite Δ^{++} baryons and negatively charged antibaryons $\bar{\Delta}^{--}$). While of course $X^{\pm\pm}$ can be added to

¹Throughout this paper we use the brackets to denote states bound by the Coulomb force.

any theory “by hand”, there is a number of BSM models where doubly charged particles make natural appearance. These include Georgi-Mahacek model, Zee-Babu model, little Higgs model and others, as surveyed in ref. [6]. How could metastability of charged BSM particles and their sizeable abundance be achieved? A recent example was presented in [10], based on the left-right symmetric models [18], and the triplet set of Higgses as an important ingredient. Among such triplet states, there are *elementary* di-charged Higgs states $\Delta_R^{\pm\pm}$. As shown in [10], a combination of the discrete symmetry $\Delta_R \rightarrow -\Delta_R$ and a certain hierarchy between the masses of BSM particles, $m_{\Delta_R} \ll m_{W_R}$, will lead to metastability of the doubly charged Higgs. Supersymmetric models, where there is a plethora of BSM charged particles, offer a general pathway to metastability of charged particles. The following mass arrangement of superpartners gives the requisite longevity within the context of a supersymmetric SM: gravitino as the lightest (LSP), and e.g. a charged superpartner of a SM lepton as the next-to-lightest superpartner (NLSP). With such mass arrangement, NLSP \rightarrow LSP decay is suppressed by the small coupling, with the decay rate suppressed by the Planck mass. This way, the lifetime of the charged NLSP can vary from seconds to many years, giving enough time for the BBN catalysis to occur. If, in addition, a supersymmetric model contains doubly charged states, then the superpartners of $X^{\pm\pm}$ (e.g. a doubly charged Higgsino $\tilde{\Delta}_R^{\pm\pm}$) can indeed be long-lived if it is the NLSP, and gravitino is the LSP. This longevity mechanism relies, of course, on the existence of the discrete R -parity. As to the significant abundance of the doubly charged states, this is relatively easy to arrange. For example, if the reheating scale is sufficiently large, reaching $T_{rh} \sim m_X$,² these particles are guaranteed to be thermalized, with subsequent freeze-out via $X^{++}X^{--} \rightarrow \text{SM}$ that will provide sufficient abundances to be probed via CBBN.

This paper is organized as follows. In the next section we discuss observational constraints on Li/Be/B abundances and quote the values that we will take as upper limits on primordial abundances. In section 3 we determine the properties of bound states of X^{--} with light nuclei and identify the important nuclear reactions. In section 4 we perform calculations, and also recast some known results, to determine the rates for the most important catalyzed reactions. In section 5 we perform the CBBN analysis of the Li/Be/B yields and set constraints on the abundance of X^{--} in a wide range of its possible lifetime. Section 6 derives abundances of anomalously heavy hydrogen and helium (i.e. of the corresponding bound states of nuclei with X^{--}). Section 7 contains the discussion and our conclusions.

2 Observational constraints of primordial Li/Be/B

Abundances of lithium, beryllium and boron are typically very small, compared not only with the main primordial elements such as hydrogen and helium, but also with star-produced elements, such as carbon and oxygen. Therefore, if the post-BBN evolution of these elements is relatively mundane, one can use their observations as a strong constraint on scenarios that deviate from the minimal (or standard) BBN (SBBN). This section contains a discussion of the values of primordial abundances of these elements that will be adopted in our study.

²We use the units $\hbar = c = k_B = 1$ throughout this paper.

We will specifically concentrate on these rare elements, as the catalytic influence of heavy charged relics on deuterium and helium is relatively mild [11].

With the rapid progress of precision cosmology in the last two decades, we now have a very accurate determination of the baryon-to-photon ratio η_B , that for a long time was one of the main uncertainty factors influencing the BBN predictions. Observations of D/H, as well as of primordial helium, are broadly consistent with the BBN predictions, at a few percent level. The comparison of observations of lithium isotopes with the corresponding SBBN predictions tells a different, and perhaps rather confusing, story.

Stable isotopes of lithium, ${}^6\text{Li}$ and ${}^7\text{Li}$, are produced in rather different amounts in SBBN. At current values of η_B , ${}^7\text{Li}$ is produced predominantly as ${}^7\text{Be}$, that much later decays to lithium via the electron capture reaction. ${}^7\text{Be}$ is produced via the mostly $E1$ -dominated (α, γ) reaction on ${}^3\text{He}$. Once produced, ${}^7\text{Be}$ proves to be rather robust against burning by protons, and its reduction by neutrons is also minimal. In contrast, the yield of ${}^6\text{Li}$ is several orders of magnitude smaller, for two reasons. The (α, γ) reaction leading to helium-deuterium fusion is very suppressed in the $E1$ channel on account of nearly same charge-to-mass ratio for D and ${}^4\text{He}$ nuclei. In addition, ${}^6\text{Li}$ undergoes very efficient burning by protons, that remains active down to very small temperatures, $T \sim 10 \text{ keV}$. Thus, the SBBN determines the resulting yields to be [19]

$$\left. \frac{{}^7\text{Li}}{\text{H}} \right|_{\text{SBBN}} = (4.94 \pm 0.72) \times 10^{-10}, \quad (2.1)$$

$$\left. \frac{{}^6\text{Li}}{\text{H}} \right|_{\text{SBBN}} \simeq 10^{-14}. \quad (2.2)$$

Other evaluations are in agreement with (2.1) within errors [20, 21].

Comparison with observations is, however, far from being straightforward. First of all, some amount of lithium is produced by CR, and the expected amount of this production mechanism, albeit with large uncertainties, by far exceeds prediction (2.2). The presence of CR predating main chemical evolution of elements in late Universe will produce ${}^6\text{Li}$ uncorrelated with metallicity, and therefore prediction (2.2) has no relevance for comparison with observations. It has to be said that the initial excitement about the claims of metallicity-uncorrelated and possibly nonstandard-BBN-induced ${}^6\text{Li}$ [22] turned out to be short-lived, as these claims have been negated by subsequent re-analyses.

Observations of ${}^7\text{Li}$ are telling another, and quite a different story. The relative constancy of ${}^7\text{Li}/\text{H}$ in the atmospheres of old and hot metal-poor stars in the Milky Way was discovered in the 1970s, and for a long time believed to be a true representation of the primordial lithium abundance [23]. This might be the case if during the ~ 13 billion years of these stars' existence there has been no significant depletion of primordial lithium in their atmospheres. Interpreted this way, the so-called Spite plateau abundance [24] is in sharp contradiction with the SBBN prediction (2.1), exhibiting a factor of 3 deficit. Latest values, as quoted in [25] and references therein, are given by

$$\left. \frac{{}^7\text{Li}}{\text{H}} \right|_{\text{Spite plateau}} = (1.6 \pm 0.3) \times 10^{-10}. \quad (2.3)$$

This discrepancy is often referred to as “primordial lithium problem”, and it has generated a great scrutiny of all its aspects, starting from re-evaluation of nuclear reaction rates to critical assessment of the assumption about lithium preservation in the atmospheres of old stars, or even various beyond-SBBN scenarios (see e.g. discussions in [25–29]).

While this is difficult to prove outright, there is a growing consensus that indeed the diffusion and gravitational settling of lithium in the atmospheres of old Population II stars may be responsible for a factor of ~ 3 depletion of lithium, from (2.1) to (2.3). Recently, it has been argued [25] that non-observation of ${}^6\text{Li}$ in amounts expected to be generated by the CR activity lends some support towards stellar depletion of both isotopes of lithium. While this may solve the ongoing discrepancy between (2.1) and (2.3), it does not answer the question of what primordial amounts of lithium current data allow. In this paper, while not attempting to address this important question in its full entirety, we try to determine the maximum amounts of ${}^6\text{Li}/\text{H}$ and of ${}^7\text{Li}/\text{H}$ that can be still consistent with observations. We will then contrast them with our CBBN predictions to derive robust limits on our model. Our interest in mass-6 isotope stems from the fact that in the CBBN version we investigate in this paper it is the catalysis of ${}^6\text{Li}$ that is most pronounced, in the limit of long lifetime for X^{--} . In carrying out the analysis, one may assume that the abundance of ${}^7\text{Li}$ is set by the standard processes — SBBN production, CR and stellar production at high metallicities, as well as possible stellar depletion. Within these assumptions, we want to *maximize* ${}^6\text{Li}/\text{H}|_{\text{BBN}}$ that can then be treated as a reasonable upper bound for the catalyzed BBN scenario.

First, we note that it is not easy to derive an upper bound on ${}^6\text{Li}/\text{H}|_{\text{BBN}}$ using the constraints on the abundance of ${}^6\text{Li}$ in the atmospheres of old stars. If ${}^7\text{Li}/\text{H}$ was indeed depleted by a factor of $\mathcal{O}(3)$, then ${}^6\text{Li}/\text{H}$ could have been depleted by a much greater factor, due to its fragility. We do not know of any reasonable way of estimating such a factor without detailed modelling of lithium diffusion/settling in the atmospheres of metal-poor stars.

An alternative route for inferring the primordial abundances that avoids Spite-type determination altogether and uses the interstellar medium (ISM) abundances of lithium and ${}^6\text{Li}/{}^7\text{Li}$ ratio has been touted (see e.g. refs. [30–33]) as a difficult but completely independent from stellar uncertainties method for inferring primordial lithium abundances. While most of the observations were performed as studies of absorption along the line of sight towards the direction of bright nearby stars [31, 33], observations of interstellar gas outside the Milky Way (in the Small Magellanic Cloud, or SMC), at quarter of the solar metallicity, have also yielded measurements of ${}^7\text{Li}/\text{H}$ and ${}^6\text{Li}/{}^7\text{Li}$ [34].

We shall consider two approaches to constraining ${}^6\text{Li}/\text{H}|_{\text{BBN}}$. The first one refers to the absolute abundances of ${}^6\text{Li}/\text{H}|_{\text{obs}}$ measured in the solar system [35], and also (with larger uncertainty) in the ISM [34]. Using these values, we can build a series of inequalities,

$$\frac{{}^6\text{Li}}{\text{H}} \Big|_{\text{BBN}} < \frac{{}^6\text{Li}}{\text{H}} \Big|_{\text{BBN}} + \frac{{}^6\text{Li}}{\text{H}} \Big|_{\text{CR}} < \mathcal{F}_{\text{max}} \times \frac{{}^6\text{Li}}{\text{H}} \Big|_{\text{obs}}. \quad (2.4)$$

Here \mathcal{F} stands for a fudge suppression factor, $\mathcal{F} > 1$, that relates the initial, BBN plus CR, abundance of ${}^6\text{Li}$ and the observed abundance:

$$\frac{{}^6\text{Li}}{\text{H}} \Big|_{\text{obs}} = \frac{1}{\mathcal{F}} \times \left(\frac{{}^6\text{Li}}{\text{H}} \Big|_{\text{BBN}} + \frac{{}^6\text{Li}}{\text{H}} \Big|_{\text{CR}} \right). \quad (2.5)$$

The factor \mathcal{F} can be written as $\mathcal{F} = \mathcal{A}\mathcal{D}$, where \mathcal{A} accounts for the suppression due to astration (cycling of the primordial gas in stars), which leads to the physical destruction of ${}^6\text{Li}$, and \mathcal{D} is the factor that takes into account adsorption of ${}^6\text{Li}$ on grains of dust, also leading to the reduced values of ${}^6\text{Li}$. To set conservative constraints on primordial ${}^6\text{Li}$, we need to *maximize* the total suppression factor \mathcal{F} by maximizing possible astration and adsorption.

For observations inside the solar system, such as in meteorites, we believe that the correction for the adsorption on dust is not particularly relevant. We can get an idea of how much stellar recycling of the initial gas has occurred from observations of deuterium in the vicinity of the solar system. Deuterium is even more fragile than ${}^6\text{Li}$, but its total suppression compared to the initial BBN value due to adsorption/astration is never larger than by a factor of 1.5 [36, 37]. This implies that we can safely assume $\mathcal{F}_{\text{max},\odot} < 2$, resulting in the following upper bound:

$$\left. \frac{{}^6\text{Li}}{\text{H}} \right|_{\text{BBN}} < 2 \times \left. \frac{{}^6\text{Li}}{\text{H}} \right|_{\odot} = 3 \times 10^{-10}. \quad (2.6)$$

Aside from the observations of lithium in stars and in the solar system, there are a few observations of lithium in the ISM. The recent measurement of ${}^7\text{Li}/\text{H}$ in SMC, ${}^7\text{Li}/\text{H}|_{\text{SMC}} = 4.8 \times 10^{-10}$, also makes a tentative determination of lithium isotopic ratio and concludes that ${}^6\text{Li}/{}^7\text{Li}|_{\text{SMC}} < 0.28$ at 3σ [34]. Comparison with other elements (K, S) in SMC and solar system allows to calibrate away the effect of the dust, and in that sense we may take into account only the astration factor, that we again assume to be not larger than 2.³ This way we derive

$$\left. \frac{{}^6\text{Li}}{\text{H}} \right|_{\text{BBN}} < 2 \times \left. \frac{{}^6\text{Li}}{\text{H}} \right|_{\text{SMC}} = 2.7 \times 10^{-10}, \quad (2.7)$$

which is a nearly the same as the value in (2.6).

Similar ballpark numbers can be achieved from older measurements of both isotopes of lithium in the ISM in proximity to solar system. However, the scatter in the results is larger than that for the measurements discussed above. Therefore, we will adopt (2.6) as a reliable and conservative limit on the maximal abundance of ${}^6\text{Li}$ that can emerge from the BBN that is consistent with solar system and ISM measurements.

One can also use solar system measurements, ${}^7\text{Li}/\text{H}$ in conjunction with D/H , to set the constraint on the maximum possible production of ${}^7\text{Li}$ in the (non-standard) BBN. This way, we get a very relaxed, and therefore quite conservative bound,

$$\left. \frac{{}^7\text{Li}}{\text{H}} \right|_{\text{BBN}} < 2 \times \left. \frac{{}^7\text{Li}}{\text{H}} \right|_{\odot} = 4 \times 10^{-9}. \quad (2.8)$$

We note that this value is about an order of magnitude larger than the SBBN one, as ${}^7\text{Li}$ in the vicinity of the solar system must have resulted from the prior CR and stellar activity. Our limit (2.8) assumes that all of it in fact came from the BBN, making it a rather conservative assumption for the purposes of limiting non-standard BBN scenarios.

³In this respect, observations of D/H in the same systems where ${}^6\text{Li}/{}^7\text{Li}$ and Li/H are measured are desirable.

Beryllium and boron are also extremely rare elements. The smallest values are found at lowest metallicities, conforming with the expectations of their secondary (not BBN) origin. Observations of these elements do not show any sign of Spite-like plateau, and if one can neglect depletion of these elements, one could derive a constraint on (nonstandard) BBN abundances of Be and B. In deriving these approximate limits, we take into account the possibility of an $\mathcal{O}(3)$ suppression of their abundance in stellar atmospheres, as for ${}^7\text{Li}$. (Unlike ${}^6\text{Li}$, these elements are less fragile than ${}^7\text{Li}$). Taking that into account and using measurements quoted in [25], we can conservatively conclude that

$$\left. \frac{{}^9\text{Be}}{\text{H}} \right|_{\text{BBN}} < 5 \times 10^{-13}; \quad \left. \frac{\text{B}}{\text{H}} \right|_{\text{BBN}} < 10^{-10}, \quad (2.9)$$

where B is understood as ${}^{10}\text{B} + {}^{11}\text{B}$. BBN contributions in excess of these values would generate Spite-like plateaus in the data, that is not seen. As we shall see, in the CBBN scenario with X^{--} the yields for these elements may be enhanced by many orders of magnitude compared with those in SBBN.

3 Properties of bound states and recombination rates

In this section we will investigate the main properties of the (NX^{--}) bound states, where N stands for a generic BBN-relevant nucleus (p , ${}^4\text{He}$, ${}^8\text{Be}$, etc.). As is well known from the CBBN studies with singly charged particles, the binding energies will be in $\mathcal{O}(\text{MeV})$ range, i.e. only marginally smaller than the nuclear binding energies relevant for BBN. The binding is achieved via the Coulomb force, and for a point-like nucleus, we would have $E_{\text{Bohr}} = Z_N^2 Z_X^2 \alpha^2 m_N / 2 = 2Z_N^2 \alpha^2 m_N$. (Notice that the reduced mass of $X^{--} - N$ system is essentially equal to m_N as $m_X \gg m_N$ ⁴). In practice, however, the bound states are never that deep, as the finite radius of the nucleus reduces the binding quite considerably, and we resort to finding the binding energies numerically.

We solve the Schrödinger equation for 2-body Coulomb problem assuming a simplistic nuclear charge distribution. We consider nuclei as uniformly charged spheres of radius $R_N = (5/3)^{1/2} r_c(N)$, where r_c is the r.m.s. charge radius. Direct check against e.g. Gaussian charge distribution reveals the stability of our results to $\mathcal{O}(\%)$ accuracy. The binding energies relevant for our study are listed in table I. These are Coulomb binding energies only, i.e. nuclear polarizability effects are not included.

Examining this table, we can make the following observations:

1. Only for proton the actual binding energy is within 1% of the Bohr formula, while for the rest of nuclei the deviation is more than 50% due to the finite charge radius. Importantly, we neglect backreaction of X^{--} on nuclear shapes, and assume the nuclei to be not deformed inside the bound states.
2. ${}^4\text{He}$ is the most abundant nucleus after p , and it forms earlier than (pX^{--}) . Recall that the usual SBBN deuterium bottleneck (the onset of nuclear reactions that uptake

⁴Note that for a generic DM-nucleus bound state this may not necessarily be true [38, 39], but here we deal with electromagnetically charged relics and very light nuclei participating in BBN.

Nucleus N	r.m.s. charge radius in fm	Binding energy in MeV
p	0.84	0.0996
${}^4\text{He}$	1.67	1.156
${}^5\text{Li}$	2.6	1.94
${}^6\text{Li}$	2.6	2.10
${}^7\text{Li}$	2.44	2.29
${}^7\text{Be}$	2.65	3.15
${}^8\text{Be}$	2.5	3.40
${}^9\text{B}$	2.5	4.61

Table 1. Coulomb binding energies for (NX^{--}) . Nuclear r.m.s. charge radii were taken from [40], except for highly unstable ${}^5\text{Li}$ and ${}^8\text{Be}$ nuclei, for which no measurements exist. For their charge radii we use extrapolated values.

n) is at $T \simeq 90$ keV, and it is ~ 25 times smaller than the deuteron binding energy of 2.2 MeV. Therefore, we can immediately conclude that the main (NX^{--}) bound states will start forming below $T \simeq 40$ keV. This will lead to significant simplifications, because only a handful of reaction are still going, and $Y_{\text{He}} = \text{const}$ at these temperatures.

3. Mass five nuclear divide (i.e. the absence of stable $A = 5$ nuclei) *is not bridged* by X^{--} . Since the rest energy excess of ${}^5\text{Li}$ compared to ${}^4\text{He} + p$ is 1.69 MeV, the $({}^5\text{Li}X^{--})$ binding energy of 1.94 MeV is not enough to compensate for that. (The relevant energy is the relative binding energy, $1.94 - 1.15 \simeq 0.8$ MeV, which is smaller than 1.69 MeV). Similar considerations and the same conclusion apply also for $({}^5\text{He}X^{--})$ bound state. Therefore, mass 5 nuclei do not form even in the binding with X^{--} , and we can ignore them.
4. Mass eight divide is definitely bridged for ${}^8\text{Be}$ and ${}^9\text{B}$, as their mass excess is $\mathcal{O}(0.1 \text{ MeV})$ while their binding energies to X^{--} are around 3 to 5 MeV. We expect that a significant fraction of X^{--} will end up in the bound states with these elements. One can also check that there is no β^+ or electron capture decay of $({}^9\text{BX}^{--})$ to $({}^9\text{Be}X^{--})$, though β^- decay $({}^9\text{Be}X^{--}) \rightarrow ({}^9\text{BX}^{--})$ is still possible.
5. Completely accidentally, our accuracy is not enough to determine the relative stability of $({}^7\text{Li}X^{--})$ vs. $({}^7\text{Be}X^{--})$. In the absence of X^{--} , ${}^7\text{Be}$ decays to lithium via electron capture, but with the calculated bindings to it, the total energies of $({}^7\text{Be}X^{--}) + e$ and $({}^7\text{Li}X^{--})$ are degenerate within a few keV, whereas we cannot trust our methods to that level. If the decay proceeds towards $({}^7\text{Li}X^{--})$, and the lifetime of X^{--} is comparable to the age of the Universe, then $({}^7\text{Li}X^{--})$, whose charge is +1, will chemically appear, after the electron recombination, as an abnormal isotope of hydrogen, while in the opposite case, the surviving state will be $({}^7\text{Be}X^{--})$ (charge +2), which will be perceived as heavy helium.
6. If X^{--} is stable on the modern Universe timescale, the abundance of $({}^6\text{Li}X^{--})$ will currently appear as abnormal hydrogen. Therefore, calculating this yield is also of interest.

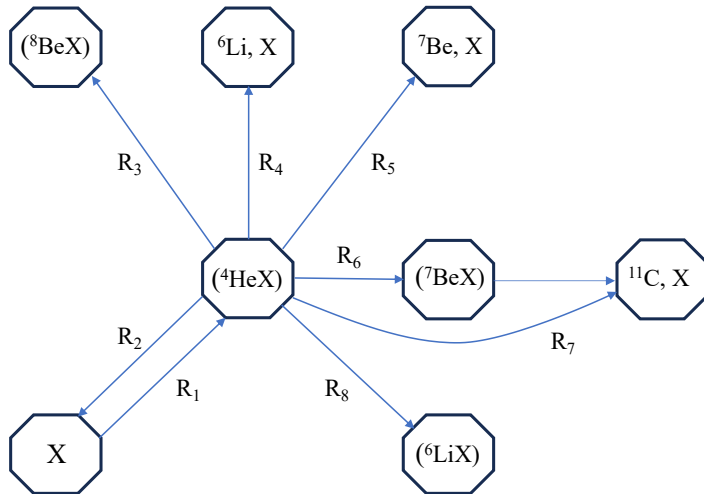


Figure 1. Schematic representation of the most relevant CBBN reactions with X^{--} . Brackets (NX^{--}) indicate a bound state of a nucleus N with X^{--} , while N, X stand for a “deconfining” transition, with the final-state N and X^{--} no longer attached to each other.

For some (NX^{--}), it turns out, we will also need to calculate the properties of their excited atomic bound states. These properties can be found again by solving the corresponding Schrödinger equations. The results should in general be even more reliable than those for the ground states, on account of a larger separation between X^{--} and the nucleus, resulting in smaller corrections due to the finite nuclear radius.

Armed with the knowledge of bound states, we can proceed to building the catalyzed BBN reaction network and calculating the yields of various elements. The key “element” for us is the bound state of X^{--} with ${}^4\text{He}$, as helium is quite abundant, and (${}^4\text{He}X^{--}$) is electrically neutral, so that its reactions with other nuclei are not suppressed by Coulomb barriers. This makes (${}^4\text{He}X^{--}$) play a central role in CBBN. The schematics of main CBBN process is given in figure 1. Our goal is to calculate or estimate the rates of the main reactions R_i and calculate the yields of ${}^6\text{Li}$, ${}^7\text{Be}$ + ${}^7\text{Li}$, and of heavier elements, such as ${}^{11}\text{B}$. The latter turns out to be mostly initially produced as ${}^{11}\text{C}$ in our case.

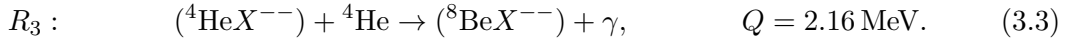
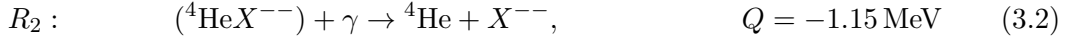
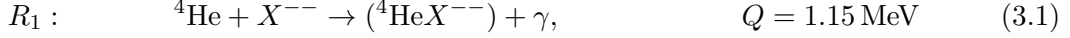
In the final states of certain reactions (R_4 , R_5 , R_7), the nuclei and X^{--} are no longer attached to each other. These are the reactions that are enhanced by the heavy charged particle X the most, as they are non-radiative and thus allow rates that are much larger than the SBBN rates [11].

Throughout our calculations, we will treat the X^{--} as a perturbation to the main SBBN reaction network, and work in the first order in their concentration. In other words, we will neglect all reactions that involve two or more of X^{--} in the initial state. This is justified, in some sense, by our results, as the constraints imposed by Li/Be/B produced in CBBN turn out to be quite strong, and the resulting maximally allowed abundances of X^{--} are indeed very small, especially for long lifetimes.

As we are going to see, the main CBBN processes are delayed until the temperatures drops below 40 keV, when the SBBN reaction are mostly complete: apart from a small leftover,

all neutrons are already incorporated into ${}^4\text{He}$. At this point of the evolution one can identify three groups of primordial elements. First, p and ${}^4\text{He}$, that have $\mathcal{O}(0.1 - 1)$ abundances, then, n , D , ${}^3\text{He}$ and T , whose abundances are in the range $\mathcal{O}(10^{-7} - 10^{-5})$. Finally, at $\mathcal{O}(10^{-10})$ and below are $\text{Li}/\text{Be}/\text{B}$. It is this last group of elements that will be affected by CBBN reactions involving X^{--} , while the first two groups are not changed by X^{--} in our approximation, and their abundances can be used as an input from the SBBN reaction network.

In the rest of this section, we consider radiative reactions R_1 , R_2 and R_3 that are most important for determining the evolution of the $({}^4\text{He}X^{--})$ bound state:



Notice that the Q -value of reaction R_3 takes into account the 92 keV mass excess of free ${}^8\text{Be}$ relative to decay into 2α .

For reactions R_1 and R_2 the calculations closely follow the standard calculations of the photoelectric effect in hydrogenic systems. It is convenient to express the cross section of $({}^4\text{He}X^{--})$ photo-disintegration reaction R_2 in the following form:

$$\sigma_{\text{photo}} = \frac{2^8 Z_{\text{He}}^2 \alpha \pi^2}{3 \exp(4) m_{\text{He}} \omega} \times \frac{\rho_{\text{rad}}^2}{\rho_{\text{rad},C}^2}. \quad (3.4)$$

In this expression, $\omega \simeq Q = 1.15 \text{ MeV}$ is the energy of the absorbed γ , $Z_{\text{He}} = 2$ is the charge of the particle that gets detached, and the last factor is the ratio of radial integral $\int r^2 dr R_{k1} R'_{10}$ calculated for realistic atomic wave functions to that for the Coulomb ones. When this ratio is set equal to unity and ω is chosen to be hydrogenic, i.e. $Z_{\text{He}}^2 Z_X^2 \alpha^2 m_{\text{He}}/2$, eq. (3.2) reduces to the textbook result for the photoelectric effect at the threshold. The cross section of the inverse (i.e.“recombination”) reaction R_1 is given by $\sigma_{\text{rec}} = \sigma_{\text{photo}} \times 2\omega^2/k_{\text{He}}^2$, where k_{He} is the momentum of the initial-state ${}^4\text{He}$. We approach these reactions in a simplified manner, and use hydrogenic wave functions, though more elaborate calculations can be performed as well. With these cross sections, we find for the rates for reactions R_1 and R_2

$$\Gamma_1(T_9) = \langle \sigma v \rangle_1 n_{\text{He}} = 0.03 \times T_9^{5/2} \text{ s}^{-1}, \quad (3.5)$$

$$\Gamma_2(T_9) = \langle \sigma v \rangle_2 n_{\gamma} = 1.88 \times 10^{15} \times T_9 \exp[-13.3/T_9] \text{ s}^{-1}, \quad (3.6)$$

where T_9 is the temperature in units of 10^9 K ($T_9 = 1$ is equivalent to $T = 86.2 \text{ keV}$). Note that Γ_1 is the rate of reaction R_1 *per one X^{--} particle*, whereas Γ_2 is the rate of R_2 *per $({}^4\text{He}X^{--})$ bound state*. These are the rates to be carried to the system of Boltzmann equations. When Γ_i ’s become larger than the Hubble expansion rate,

$$H(T_9) = 2.8 \times 10^{-3} \times T_9^2 \text{ s}^{-1}, \quad (3.7)$$

the corresponding reactions tend to approach equilibrium. It is easy to see that $\Gamma_1 > H$ for all $T_9 < 1$, and it is the rapidly falling with T rate of R_2 that determines the survival of $({}^4\text{He}X^{--})$. This is, of course, in direct analogy with the delayed SBBN deuterium formation, and it is appropriate to call it “the $({}^4\text{He}X^{--})$ bottleneck”.

Another very important reaction for CBBN is R_3 , as it removes (${}^4\text{He}X^{--}$) and hides X^{--} behind the Coulomb barrier of beryllium, making all subsequent reactions with it inefficient. Therefore an accurate evaluation of its rate has to be done. The overall rate of R_3 is given by a combination of the resonant and non-resonant parts. We will use the following strategy for calculating the resonant part of this rate, corresponding to the channel $({}^4\text{He}X^{--}) + {}^4\text{He} \rightarrow ({}^8\text{Be}X^{--})^* \rightarrow ({}^8\text{Be}X^{--}) + \gamma$. The intermediate ($\text{Be}X^{--}$) in this reaction has the excited $n = 3, l = 1$ Coulomb bound state with the excitation energy 1.11 MeV, which is almost exactly at the $({}^4\text{He}X^{--}) + {}^4\text{He}$ separation threshold, with $\Delta E = 0.13$ MeV. (These energy values were found numerically by solving the corresponding Schrödinger equation.) This is a well known narrow resonance situation, when the reaction rate is determined by the relative magnitude of the entrance channel width Γ_{in} and the exit channel width Γ_{out} . The entrance width drops out as long as it is larger than the exit width but is smaller than temperature. For the reaction we consider, this is actually the case. Indeed, the entrance width Γ_{in} for reaction R_3 is set by strong and electromagnetic non-radiative processes, and we estimate it to be in the ~ 100 eV – 1 keV range. Thus, it is expected to be much larger than the photon emission widths, which for bound states of X^{--} with light nuclei can reach $\mathcal{O}(\text{eV})$. The resonant contribution to the reaction rate should therefore be determined by the exit rate, which is the rate of radiative de-excitation of $n = 3$ excited Coulomb state of (${}^8\text{Be}X^{--}$): $\Gamma_{\text{out}} = \Gamma_{({}^8\text{Be}X^{--}),n=3 \rightarrow ({}^8\text{Be}X^{--}),n=1,2}$. This gives

$$\langle \sigma v \rangle_{3,\text{res}} = \left(\frac{2\pi}{T m_{\text{He}}} \right)^{3/2} 3\Gamma_{\text{out}} \exp[-\Delta E/T] \rightarrow \Gamma_{3,\text{res}} = 0.43 \times \exp[-1.64/T_9] \times T_9^{3/2} \text{s}^{-1}. \quad (3.8)$$

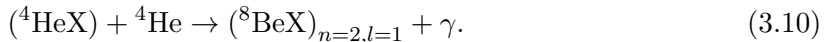
In obtaining the last expression we used

$$\Gamma_{\text{out}} = \Gamma_{3p \rightarrow 2s} + \Gamma_{3p \rightarrow 1s} = \sum_{1s,2s} \frac{4}{9} Z_{\text{Be}}^2 \alpha \omega_{\gamma}^3 |\langle r \rangle|^2 \simeq 6 \text{ eV}, \quad (3.9)$$

where the energies ω_{γ} of the radiative transitions and the transition radial matrix elements $\langle r \rangle$ were calculated numerically.

In principle one could also add contributions of other resonances, such as $l = 2$ and $l = 0$ $n = 3$ intermediate states, but it turns out that $l = 2$ state is ~ 190 keV sub-threshold, and for $n = 3, l = 0$ state the resonance is 230 keV above threshold, so that we can ignore them both. Also, importantly, the inverse reaction can be ignored, as very few photons of sufficient energy exist at $T_9 < 0.5$. We can observe that the resonant rate of forming (${}^8\text{Be}X^{--}$) is fairly large at $T_9 \sim 0.3$, but it falls off quickly with temperature.

To estimate the late-time removal of (${}^4\text{He}X^{--}$) via the formation of (${}^8\text{Be}X$), we need to know the non-resonant part to the rate of R_3 . Going to extremely slow initial particles, one could argue that the s -wave scattering should dominate, and therefore the following capture reaction must occur,



The p -wave final state is uniquely determined by requiring that the reaction be exothermic and by the dominance of $E1$ amplitude. The *intermediate* energy release in this reaction

is given by the energy differences

$$\omega_\gamma = Q = (-1.15 \text{ MeV} - (-2.24 \text{ MeV} + 0.09 \text{ MeV})) = +1.00 \text{ MeV}, \quad (3.11)$$

where 2.24 MeV is the $2p$ binding energy between ${}^8\text{Be}$ and X^{--} .

The calculation of the non-resonant contribution to the rate of R_3 is a complicated 3-body problem, but what simplifies it is that the interaction with photon can be treated as perturbation. The cross section for this reaction can be approximated as

$$\sigma v = \frac{\alpha Z_{\text{He}}^2 \omega_\gamma^3}{2\pi} \sum_\lambda \int d\Omega_\gamma \left| \int d^3 r_1 d^3 r_2 \psi_{\text{Be}X}^* \left(\frac{\vec{r}_1 + \vec{r}_2}{2} \right) \psi_{\text{Be}}^* (|\vec{r}_1 - \vec{r}_2|) \right. \\ \left. \times \vec{\epsilon}_\lambda \cdot (\vec{r}_1 + \vec{r}_2) \psi_{\text{He}X} (\vec{r}_1) \psi_{\text{He}} (\vec{r}_2) \right|^2, \quad (3.12)$$

where $\vec{\epsilon}_\lambda$ is the polarization vector of the outgoing photon. The heavy X particle is located at the origin, and the coordinates of α particles are \vec{r}_1 and \vec{r}_2 . The electric dipole operator in this system is proportional to $\vec{r}_1 + \vec{r}_2$. This is a simplified α -cluster picture of ${}^8\text{Be}$ as being a bound state of two ${}^4\text{He}$ nuclei in the relative s -wave. $\psi_{\text{He}} (\vec{r}_2)$ is asymptotically the plane wave $\exp(i\vec{k}\vec{r}_2)$ of the incoming α -particle with momentum $k \sim \sqrt{T M_{\text{He}}}$, which corresponds to $k^{-1} \sim 20 \text{ fm}$. Thus, one can use the long-wavelength approximation for the incoming ${}^4\text{He}$. $\psi_{\text{He}X} (\vec{r}_1)$ and $\psi_{\text{Be}X} \left(\frac{\vec{r}_1 + \vec{r}_2}{2} \right)$ are the bound state wave functions that we have found numerically, taking into account the finite nuclear sizes. Many of the remaining integrals can be done analytically, exploiting the orbital properties (s -wave or p -wave) of the bound states. The summation over the photon polarizations and integration over its directions is also done analytically. The final part of the calculation is performed *assuming* a certain form of the 2α wave function inside ${}^8\text{Be}$, which we take to be Gaussian, with the widths reproducing the expected charge radius of ${}^8\text{Be}$. We also varied this shape, to make sure we are not overly dependent on our assumptions. As a result, we arrived at the following estimate for the non-resonant part of the cross section:

$$\sigma v / c \simeq (3 - 9) \times 10^{-31} \text{ cm}^2. \quad (3.13)$$

Eventually, to get the *conservative* bounds on lifetime and abundance of X^{--} , we need to take the maximum rate for R_3 , and therefore we adopt the largest value of the cross section in (3.13), which yields

$$\Gamma_{3,\text{non-res}} \simeq 0.02 \times T_9^3 \text{ s}^{-1}. \quad (3.14)$$

The sum of the (3.8) and (3.14) gives our final estimate for Γ_3 , which for $T_9 \simeq 0.2 - 0.4$ is only marginally smaller than Γ_1 .

4 Catalyzed reactions

Once the (${}^4\text{He}X^{--}$) state is formed, it can react in a variety of ways. As already mentioned, R_3 removes some of these states from the play and hides them inside (${}^8\text{Be}X^{--}$) that can further transform to (${}^9\text{BX}^{--}$). It is interesting that if X^{--} is unstable, these extra bound

states are relatively harmless, as outside the bound states they immediately decay to 2α and $p2\alpha$. It has to be mentioned that the reaction $(^8\text{Be}X^{--}) + n \rightarrow ^9\text{Be} + X^{--}$ has a negative Q -value and can be neglected. This is in contrast with CBBN with singly charged particles, where such reaction is catalyzed [41, 42]. The rate for the (n, γ) reaction on $(^8\text{Be}X^{--})$ will be of course additionally suppressed. Therefore, the reactions of $(^4\text{He}X^{--})$ with other elements, pictured in figure 1, that are of most interest to us, are

$$R_4 : \quad (^4\text{He}X^{--}) + \text{D} \rightarrow X^{--} + {}^6\text{Li}, \quad Q = 0.31 \text{ MeV} \quad (4.1)$$

$$R_5 : \quad (^4\text{He}X^{--}) + {}^3\text{He} \rightarrow X^{--} + {}^7\text{Be}, \quad Q = 0.41 \text{ MeV} \quad (4.2)$$

$$R_6 : \quad (^4\text{He}X^{--}) + {}^3\text{He} \rightarrow (^7\text{Be}X^{--}) + \gamma, \quad Q = 3.56 \text{ MeV} \quad (4.3)$$

$$R_7 : \quad (^4\text{He}X^{--}) + {}^7\text{Be} \rightarrow {}^{11}\text{C} + X^{--}, \quad Q = 6.39 \text{ MeV} \quad (4.4)$$

$$R_8 : \quad (^4\text{He}X^{--}) + \text{D} \rightarrow (^6\text{Li}X^{--}) + \gamma, \quad Q = 2.42 \text{ MeV}. \quad (4.5)$$

We could also include other reactions, e.g. with ${}^3\text{H}$, but by the time $(^4\text{He}X^{--})$ is formed, tritium concentration is already considerably depleted.

Before performing any calculations, we note that the rates for the first two reactions here dominate, $\Gamma_{4,5} \gg \Gamma_{6,7,8}$. Reaction R_7 is catalyzed, but its rate is suppressed due to the small SBBN abundance of ${}^7\text{Be}$, while $R_{6,8}$ are radiative, which leads to suppression of their rates. We still need reaction R_8 for the following reason: for a very long-lived X^{--} , $\tau_X > 13 \text{ bn yr}$, its bound state with ${}^6\text{Li}$ will appear as a super-heavy isotope of hydrogen.

In order to get estimates for the rates of $R_{4,5}$, we use the previously calculated rates for reactions with singly charged X^- . In particular, ref. [43] evaluates $(^4\text{He}X^-) + \text{D} \rightarrow {}^6\text{Li} + X^-$ and $(^4\text{He}X^-) + {}^3\text{He} \rightarrow {}^7\text{Be} + X^-$, finding the astrophysical S -factors for both. We make the assumption that the S -factors remain roughly the same for X^{--} and, taking into account that $(^4\text{He}X^{--})$ is electrically neutral, rescale the rates found in [43] by “stripping off” the Coulomb barrier penetration factor \mathcal{P} . This factor can be written as

$$\mathcal{P} = \sqrt{\frac{E_G}{E}} \exp\left(-\sqrt{\frac{E_G}{E}}\right), \quad (4.6)$$

where E_G is the Gamow energy for the reaction with singly-charged X^- , $E_G = 2\pi^2\alpha^2 Z_N^2 m_N$. Here m_N is the mass of the incoming nucleus, m_{D} for reaction (4.1) and $m_{^3\text{He}}$ for reaction (4.2).

We also need to take into account Sommerfeld/Coulomb enhancement in the final state, described by the factor

$$\mathcal{C}(Z_X) = \frac{2\pi Z_X Z_N \alpha}{v}. \quad (4.7)$$

This quantity is actually Q -value dependent, as $v = \sqrt{2Q/m_N}$. To properly rescale the results of [43], we need to multiply them by $\mathcal{C}(Z_X = 2)/\mathcal{C}(Z_X = 1)$. Numerically, we find that for reactions R_4 and R_5 these rescaling factors are 3.9 and 3.5, respectively.

Putting it all together, one gets the following approximate formula:

$$\langle\sigma v\rangle_{4(5)} = \frac{\mathcal{C}(2)}{\mathcal{C}(1)} \frac{S_{4(5)}}{\sqrt{E_G m_N / 2}}. \quad (4.8)$$

This expression is velocity-independent in the limit of small velocity, as it should be. The S -factors here correspond to catalysis with singly charged X^- ; following [43], we take S to be $\simeq 45$ b keV for reaction R_4 and $\simeq 15$ b keV for reaction R_5 .

We can now evaluate the corresponding quantities and reaction rates. In the standard notation for the reaction rates, we obtain the following expressions:

$$\lambda(R_4) \equiv N_A(\sigma v)_4 = 6.9 \times 10^7 \text{ cm}^3 \text{ s}^{-1} \text{ mole}^{-1}, \quad (4.9)$$

$$\lambda(R_5) \equiv N_A(\sigma v)_5 = 7.3 \times 10^6 \text{ cm}^3 \text{ s}^{-1} \text{ mole}^{-1}, \quad (4.10)$$

where N_A is the Avogadro constant. This gives the following rates per $(^4\text{He}X^{--})$ to be used in the Boltzmann BBN network:

$$\Gamma_4 = (\sigma v)_4 n_{\text{D}} = 0.03 \times T_9^3 \text{ s}^{-1}, \quad (4.11)$$

$$\Gamma_5 = (\sigma v)_5 n_{^3\text{He}} = 1.1 \times 10^{-3} \times T_9^3 \text{ s}^{-1}. \quad (4.12)$$

Here we used the SBBN abundances of D and ^3He . (In fact, Γ_4 gets additional mild evolution with temperature, as D/H is still a slow-varying function of temperature below $T_9 = 0.4$.) Very importantly, Γ_5/H stays above 1 until $T_9 = 0.08$, which guarantees very large output of ^6Li per X^{--} .

We can further assess the rates for other reactions of interest. Consider first reaction R_6 (4.3). If X^{--} is stable on the timescale of the age of the Universe, and if $(^7\text{Be}X^{--})$ does not decay to $(^7\text{Li}X^{--})$, it should currently appear as a heavy isotope of He, just as $(^8\text{Be}X^{--})$ does. However, its abundance is much smaller than that of $(^8\text{Be}X^{--})$, hence reaction R_6 can be safely ignored in this case. If X^{--} is unstable, then, after the decay of X^{--} , $(^7\text{Be}X^{--})$ gives a contribution to ^7Be , and ultimately to ^7Li . The rate of R_6 can therefore be added to that of R_5 and, since $\Gamma_6 \ll \Gamma_5$, we do not consider it further.

The rate of reaction R_7 is not known. However, we can make a crude estimate for this rate by assuming that ^7Be and ^4He coalesce into ^{11}C with the cross section $\sim \pi(R_{\text{He}} + R_{\text{Be}})^2 v_0/v$, where $v_0 \sim Z_{\text{He}}\alpha$ is the characteristic velocity of helium on its orbit in $(^4\text{He}X^{--})$ and v is the relative velocity of the colliding $(^4\text{He}X^{--})$ and ^7Be . This yields

$$(\sigma v)_7 \sim 2.5 \times 10^{-26} \times c \quad \rightarrow \quad \Gamma_7 = (\sigma v)_7 \times n_{\text{Be}_7} = 3.5 \times 10^{-6} T_9^3 \text{ s}^{-1}. \quad (4.13)$$

Here n_{Be_7} stands for the SBBN number density of ^7Be . Notice that $\Gamma_7/H \ll 1$ at all times due to the extremely small SBBN abundance of ^7Be . Therefore, the output of ^{11}C per X^{--} will remain small. The production of ^{11}C will, however, have the following interesting consequence. ^{11}C is virtually stable at the BBN temperatures, and it has a delayed decay to ^{11}B . Therefore, a significant fraction of newly created ^{11}B will be shielded from the proton-induced burning. Weak decay of ^{11}C and reaction $^{11}\text{B} + p \rightarrow 3\alpha$ are added to our CBBN reaction network with the standard values of their rates (see e.g. [44]).

Finally, the rate of reaction R_8 that determines the abundance of stable $(^6\text{Li}X^{--})$ when X^{--} is stable on the timescale of $\gtrsim 13$ bn years can be estimated from the following considerations. While this is a photon emission rate and therefore it is several orders of magnitude below that of reaction R_4 , it is still much enhanced compared with the rate of the SBBN reaction $^4\text{He} + \text{D} \rightarrow ^6\text{Li} + \gamma$. The reason is that the $(^4\text{He}X^{--}) + \text{D}$ system does

have an unsuppressed $E1$ dipole operator $\vec{d} = Z_{De} \times \vec{r}_D$, and therefore one should expect this reaction to have a Coulomb-unsuppressed rate characteristic for $E1$ transitions. More specifically, we expect that the replacement of ${}^4\text{He}$ by $({}^4\text{He}X^{--})$ amounts to the enhancement of the $E1$ amplitudes by the factor

$$\mathcal{S} = \frac{|\vec{d}_{({}^4\text{He}X^{--})-\text{D}}|}{|\vec{d}_{\text{D}-\text{D}}|} = \frac{m_\alpha + m_D}{m_D m_\alpha} \times \left(\frac{2}{m_\alpha} - \frac{1}{m_D} \right)^{-1} \simeq 230. \quad (4.14)$$

To estimate the rate for R_8 , we use the calculations of $E1$ -induced transition in the standard ${}^4\text{He}+\text{D}$ fusion, ref. [45], that gives $\sigma_{D(\alpha,\gamma){}^6\text{Li}}$ on the order of $0.5 \times 10^{-33} \text{ cm}^2$ at 1.5 MeV . We then apply the following rescaling, taking into account that the cross section for R_8 scales as v^{-1} in the limit of small velocities:

$$(\sigma v)_8 = \mathcal{S}^2 \times (\sigma_{D(\alpha,\gamma){}^6\text{Li}} v)_{E=1.5 \text{ MeV}} \sim 1 \times 10^{-30} \text{ cm}^2 \times c. \quad (4.15)$$

We note that this is quite a typical size for the Coulomb-unsuppressed cross section with $E1$ photon emission. This way we arrive at the reaction rate for R_8 ,

$$\Gamma_8 = (\sigma v)_8 \times n_D \simeq 8 \times 10^{-6} T_9^3 \text{ s}^{-1}, \quad (4.16)$$

where we used the SBBN value for deuterium concentration n_D . As expected, this rate is below the Hubble expansion rate.

5 CBBN yields of Li/Be/B

Having determined the most relevant catalyzed rates, we can build the CBBN reaction network, assuming X^{--} to be a small linear perturbation, and following the fate of the bound states and the catalyzed Li/Be/B production.

The evolution of the bound states of X^{--} is shown in figure 2. The process of their formation indeed starts at $T_9 < 0.4$, and most doubly charged particles end up inside these bound states. With our estimate of the non-resonant part of Γ_3 , we conclude that most (about 80%) of X^{--} end up inside $({}^8\text{Be}X^{--})$, while only about 20% are preserved in the form of highly reactive $({}^4\text{He}X^{--})$. Should we completely neglect the non-resonant part of R_3 , the balance would shift towards $({}^4\text{He}X^{--})$, as it reaches 90% in that case. Still, this uncertainty is acceptable, as it shows that indeed under any assumptions large quantities of $({}^4\text{He}X^{--})$ per X^{--} are preserved.

It is instructive to discuss also the subsequent fate of the free X^{--} . At temperatures below $T_9 \sim 0.03$ they will start forming bound states with protons, $p + X^{--} \rightarrow (pX^{--}) + \gamma$. This is followed by the extremely fast charge exchange reaction with helium (as was investigated for singly charged relics in [42]), $(pX^{--}) + {}^4\text{He} \rightarrow ({}^4\text{He}X^{--}) + p$. This completely eliminates the population of free X^{--} , but is not relevant for our discussion as it has only a minor effect on the $({}^4\text{He}X^{--})$ abundance.

Next, we investigate the yields of Li/Be/B, upon the inclusion of all CBBN rates. At this point we will keep the lifetime of X^{--} as a variable, and analyze the outcome as a function of τ_X . Figure 3 shows the evolution curves for the main elements we are interested in. As is clearly visible in the figure, the abundance of ${}^6\text{Li}$ is initially rather suppressed because of the

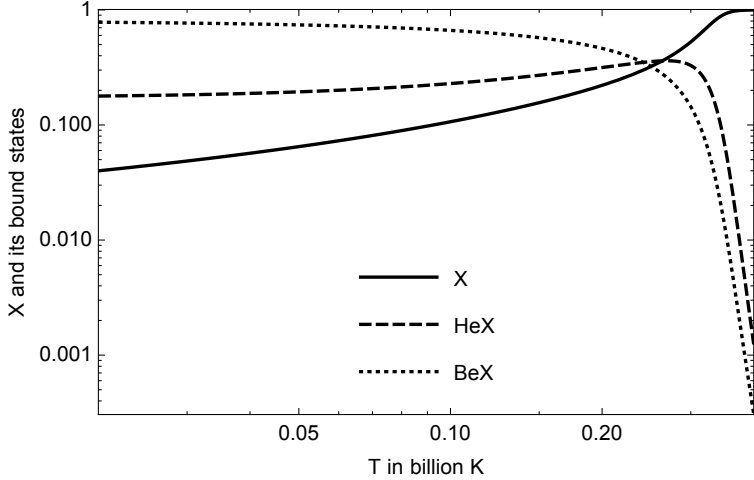


Figure 2. Evolution of X^{--} and of its bound states in the limit of parametrically long lifetime. The sum of all concentrations here is equal to one by definition. The graph shows that the main uptake of X^{--} happens below $T = 30$ keV, and $(^8\text{Be}X^{--})$ eventually absorbs about 80% of doubly negatively charged particles. 20% remain in the most reactive form $(^4\text{He}X^{--})$. The concentration of free X^{--} drops to a few percent level mark.

very efficient (p, α) burning of this element. However, at $T_9 \sim 0.1$ this burning stops, and the yield of ${}^6\text{Li}$ comes to dominate the Li/Be/B BBN predictions. Boron and ${}^7\text{Be}$ in that sense are relatively suppressed. Despite the fact that the formation of ${}^6\text{Li}$ is Coulomb-unsuppressed, at certain point it still decouples, simply because the corresponding rate, weighted by the Hubble rate, drops with temperature, $\Gamma_4/H \sim T_9$. The small temperature limit of the curves in figure 3 allows us to determine the yields of the relevant elements per X^{--} particle. Thus, for parametrically long lifetimes $\tau_X \gg \tau_{\text{BBN}}$ we get the following freeze-out yields:

$$\frac{{}^6\text{Li}}{X^{--}} \simeq 0.25; \quad \frac{{}^7\text{Be}}{X^{--}} \simeq 0.04; \quad \frac{{}^{11}\text{B}}{X^{--}} \simeq 0.7 \times 10^{-4}. \quad (5.1)$$

Now we can compare these predictions with the observational limits on the ${}^6\text{Li}$ abundance, eq. (2.6), and we immediately conclude that X^{--}/H must satisfy

$$\left. \frac{X^{--}}{\text{H}} \right|_{\tau_X \gg \tau_{\text{BBN}}} < 10^{-9}. \quad (5.2)$$

This is a much stronger limit, by about four orders of magnitude, than the one previously found for X^- , which is mostly due to the absence of the Coulomb barrier for $(^4\text{He}X^{--})$.

One example of the yields of Li/Be/B for a finite lifetime of the X^{--} particles is given in figure 3, lower panel, where the lifetime is chosen to be 500 seconds. In that case the production of Li/Be/B stops early, as there is no late time abundance of X particles, and nearly all ${}^6\text{Li}$ is burnt. However, ${}^7\text{Be}$ is preserved, and its yield is $\sim 10^{-3}$ per X^{--} particle. Using the conservative upper limit on ${}^7\text{Li}$ production in BBN (2.8) will limit the initial abundance of X^{--} to be less than 10^{-5} . (The initial abundance here is defined as $(X^{--}/\text{H})|_{t \ll t_{\text{BBN}}}$).

Generalizing this to arbitrary lifetimes of the X^{--} particles, we derive the constraints on their initial abundance. The upper panel of figure 4 gives the yields of ${}^6\text{Li}/\text{H}$ and ${}^7\text{Be}/\text{H}$.

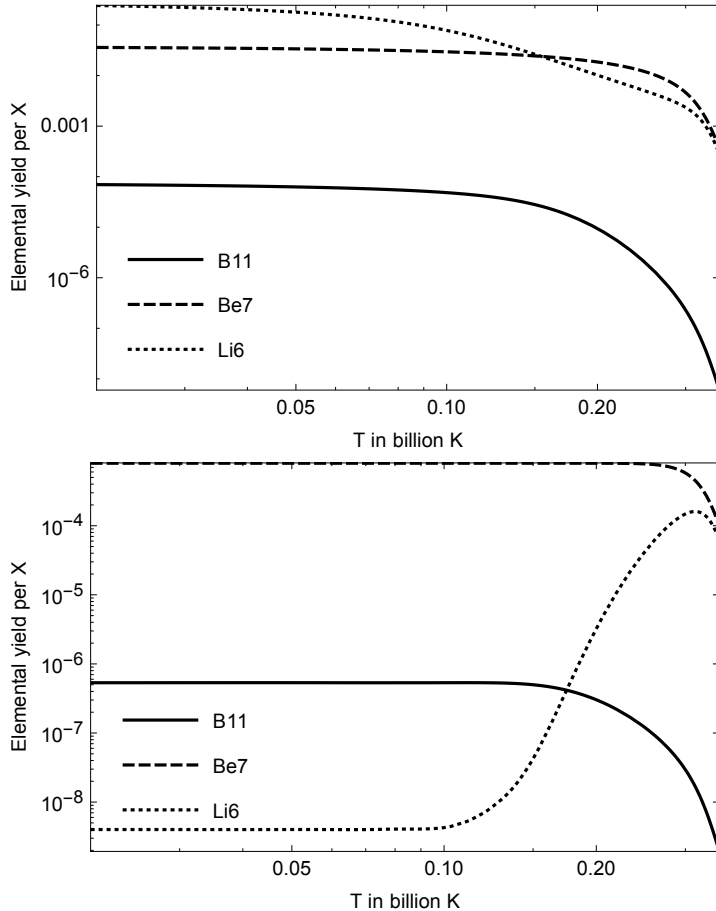


Figure 3. *Upper panel:* yields of Li/Be/B for very long lifetime of X^{--} . The left ends of the curves give the freeze-out values for the elements, *per X^{--} particle*. As expected, ${}^6\text{Li}$ dominates the exotic BBN yields. *Lower panel:* same but for the finite lifetime, $\tau_X = 500\text{ s}$. The suppression of ${}^6\text{Li}$ is apparent, and the main result of the catalysis is production of ${}^7\text{Be} \rightarrow {}^7\text{Li}$.

Taking into account that free ${}^7\text{Be}$ becomes ${}^7\text{Li}$ and making use of the conservative limits on ${}^6\text{Li}$ and ${}^7\text{Li}$ from section 2, eqs. (2.6) and (2.8), we plot the resulting limits on the X^{--}/H abundance in the lower panel of the same figure. As expected, the constraint loses its power for short lifetimes, $\tau_X < 100\text{ s}$. For lifetimes $\tau_X < 2500\text{ s}$, ${}^7\text{Li}$ data have more constraining power, while for longer lifetimes ${}^6\text{Li}$ is more important.

6 Constraints from searches for heavy isotopes of H and He

If X -particles are stable or practically stable (i.e. if their lifetime is comparable to or larger than the age of the Universe), doubly positively charged X^{++} would currently appear as an anomalously heavy isotope of He. Bound state of $({}^8\text{Be}X^{--})$ should chemically behave in exactly the same way. We predicted, figure 2, that the relative abundance of these states will be significant, $({}^8\text{Be}X^{--})/X^{--} \sim \mathcal{O}(1)$. We also found that a small fraction of ${}^6\text{Li}$ (and possibly ${}^7\text{Li}$) will end up in bound states with X^{--} . Such states would currently appear chemically as anomalously heavy isotopes of hydrogen.

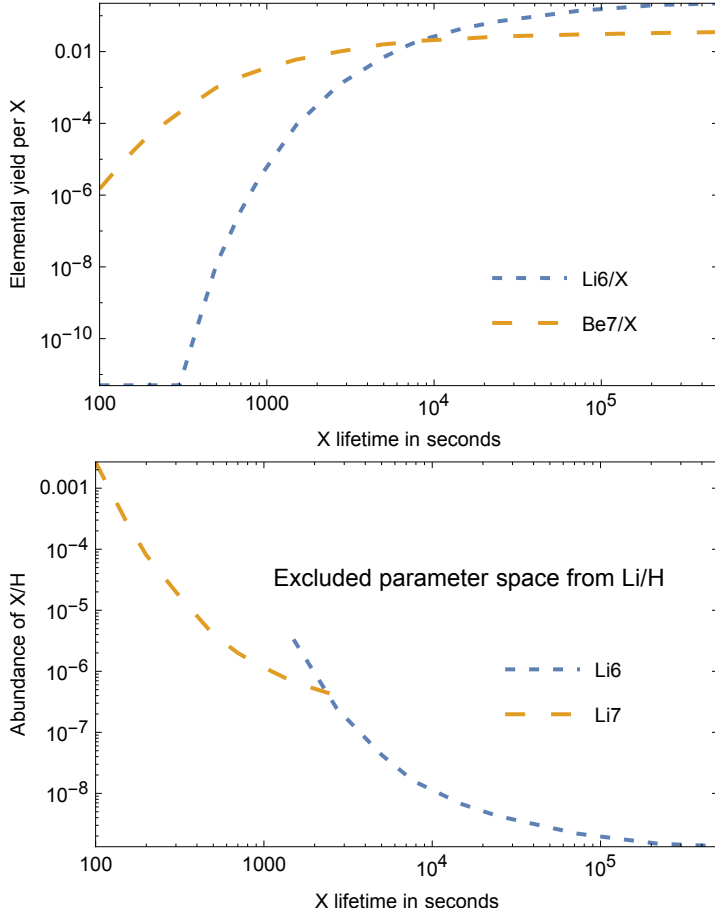


Figure 4. *Upper panel:* CBBN production of ${}^6\text{Li}$ and ${}^7\text{Be}$ as a function of the lifetime of X^{--} . ${}^6\text{Li}$ yield is larger by a factor of a few at long lifetimes. At short lifetimes, the yield of ${}^7\text{Be}$ significantly exceeds that of ${}^6\text{Li}$. *Lower panel:* constraints from observations of ${}^7\text{Li}$ and ${}^6\text{Li}$ (eqs. (2.8) and (2.6)) on the initial abundance X^{--}/H .

Bound states of the X -particles can come to the Earth with CR, or be present at the time of formation of the Earth. Therefore, their abundances should be subject to constraints coming from terrestrial searches of abnormally heavy isotopes of He and H.

Search for anomalously heavy helium in the Earth's atmosphere was carried out using the laser spectroscopy technique in [15], and the limit $10^{-12} - 10^{-17}$ per atom over the mass range $20 - 10^4$ GeV was obtained. In the scenario with doubly charged X -particles, it can be directly translated into the corresponding limit on the abundance of X^{--} :⁵

$$\left. \frac{({}^8\text{Be}X^{--})}{\text{H}} \right|_{\tau_X > \tau_{\text{Universe}}} \sim \left. \frac{X^{--}}{\text{H}} \right|_{\tau_X > \tau_{\text{Universe}}} < 10^{-12} - 10^{-17} \quad (10^2 \text{ GeV} < m_X < 10^4 \text{ GeV}). \quad (6.1)$$

This constraint is manifestly much stronger than any CBBN bounds one may derive, but, unlike the latter, it is applicable only in the $100 - 10^4$ GeV mass window.

⁵We note that doubly charged long-lived particles with mass $m_X < 100$ GeV are definitely excluded on account of various collider constraints.

A comment on the upper border of this mass interval is in order. The study in [15] exploited the isotopic shift of the atomic lines and high volatility of normal helium as opposed to much reduced volatility of anomalously heavy isotopes. One can expect that the constraint should apply as long the mass is not larger than a critical one: at very large m_X , the gravitational settling velocity of anomalous helium will be larger than the typical convective velocities in the atmosphere. Due to large atomic-size cross sections, such mass may reach rather high values. Ref. [15] believes that above $m_X > 10^4$ GeV, the efficiency of heavy helium extraction drops, and the limits will become uncertain.

As mentioned above, the existence of long-lived X^{--} will also imply the existence of abnormally heavy hydrogen isotopes, ($\text{Li}X^{--}$). We have already pointed out that within the accuracy of our approach it is not possible to determine with certainty whether (${}^7\text{Li}X^{--}$) or (${}^7\text{Be}X^{--}$) is stable, due to their accidental near degeneracy. If (${}^7\text{Be}X^{--}$) is stable, then (${}^7\text{Li}X^{--}$) will beta-decay to it, contributing to anomalous helium. In the opposite case, (${}^7\text{Be}X^{--}$) will undergo a weak electron capture to (${}^7\text{Li}X^{--}$), becoming chemically equivalent to anomalous hydrogen. Due to this uncertainty, we resort to estimating the abundance of (${}^6\text{Li}X^{--}$), which will remain stable once the temperature drops to $T_9 < 0.1$.

The bound state (${}^6\text{Li}X^{--}$) can be generated via several pathways. One of them is reaction R_8 , eq. (4.5). Another pathway involves the charge exchange reaction

$$({}^4\text{He}X^{--}) + {}^6\text{Li} \rightarrow ({}^6\text{Li}X^{--}) + {}^4\text{He}. \quad (6.2)$$

While the cross section of this reaction is very large (\sim geometric), the overall abundance of ${}^6\text{Li}$ is tiny, and we expect the (D,γ) reaction (4.5) to dominate.

Using (4.16), we estimate the yield of (${}^6\text{Li}X^{--}$) to be

$$\left. \frac{({}^6\text{Li}X^{--})}{X^{--}} \right|_{\tau_X > \tau_{\text{Universe}}} \simeq \frac{({}^4\text{He}X^{--})}{X^{--}} \times \int_0^{T_9=0.1} \frac{\Gamma_8 dT_9}{T_9 H(T_9)} \simeq 5 \times 10^{-5}. \quad (6.3)$$

In ref. [16] search for abnormal hydrogen isotopes in water was carried out using mass spectrometry methods, and the upper bound of $10^{-28} - 10^{-29}$ per nucleon in the mass range $m_X = 12 - 10^3$ GeV was established. Together with the estimate (6.3), it implies

$$\left. \frac{X^{--}}{\text{H}} \right|_{\tau_X > \tau_{\text{Universe}}} < 10^{-23} - 10^{-24} \quad (12 \text{ GeV} < m_X < 10^3 \text{ GeV}). \quad (6.4)$$

Note, however, that this constraint is applicable in a rather narrow interval of m_X , a significant portion of which has now been excluded by collider data.

In ref. [17] search was performed for abnormally heavy hydrogen isotopes in sea water, using centrifugation followed by atomic spectroscopy technique. The upper limit of 6×10^{-15} relative to normal hydrogen was obtained for the mass interval $10^4 - 10^8$ GeV. Together with (6.3), this gives

$$\left. \frac{X^{--}}{\text{H}} \right|_{\tau_X > \tau_{\text{Universe}}} < 10^{-11} \quad (10^4 \text{ GeV} < m_X < 10^8 \text{ GeV}). \quad (6.5)$$

Though this constraint is significantly weaker than that in eq. (6.4), it is applicable in a substantially wider interval of m_X .

While the limit in eq. (6.4) is demonstratively stronger than (6.1) (within its range of sensitivity to m_X), one has to keep in mind that it is at the same time less certain; the same also applies to constraint (6.5). Indeed, while abnormal helium is chemically inert, abnormal hydrogen isotopes will have a lot more complicated chemistry due to the presence of the valence electron. Therefore, while less stringent than (6.4), eq. (6.1) is more robust against chemical evolution alteration of terrestrial abundance of $(\text{Li}X^{--})$. It is also not clear how both limits should be interpreted for masses heavier than $\sim 1 - 10 \text{ TeV}$, as several assumptions built into these constraints would not hold.

For an extensive review and discussion of non-collider searches of heavy stable particles see ref. [46] and references therein.

7 Discussion and conclusions

We have derived the yields of Li/Be/B from the presence of X^{--} particles during the BBN. Our results should be considered rather conservative, as we took very relaxed observational upper bounds on the maximum yields of ${}^6\text{Li}$ and ${}^7\text{Li}$ during BBN. The accuracy of our predictions is not believed to be better than a factor of a few, however, as they partly rely on the rescaling of the catalyzed nuclear rates for singly charged particles. In order to achieve a more accurate result, one may want to repeat the corresponding calculations for X^{--} rather than X^- . However, for the log-log plot of figure 4, these uncertainties are tolerable, and they cannot change the overall picture of a huge enhancement of the ${}^6\text{Li}$ and ${}^7\text{Be}$ yields in CBBN. The strength of the CBBN limit at asymptotically long lifetimes, $X^{--}/\text{H} < 10^{-9}$, allows to conclude that the energy injection during the CMB epoch due to e.g. continuing R_3 reaction is not going to provide additional constraints. Indeed, the best CMB sensitivity is at the level of $\mathcal{O}(10^{-2} \text{ eV})$ of energy injected per baryon, which is significantly lower than continuing reactions with $({}^4\text{He}X^{--})$ can provide, once (5.2) is implemented.

We shall discuss now some implications of our results. A crucial aspect of the cosmological scenario is the initial temperature of the Universe T_{rh} , which is believed to be generated in the process of reheating after inflation. If the T_{rh} is comparable to or larger than $\sim 0.05m_X$, one can count on a sizeable abundance of X^{--} , as charged particles at these temperatures are guaranteed to stay in thermal equilibrium. Subsequent cooling ensures that $X^{--} + X^{++}$ annihilation into the SM states (charged particle pairs or photon pairs, for example) will lead to a freeze-out abundance of X^{--} that should be treated as an *initial* abundance for our BBN calculations. Due to large mass of X the annihilation cross sections are of a natural electroweak size. As a result, despite the annihilation, a significant remainder of X -particles will be preserved.

An alternative possibility is the scenario where T_{rh} is below m_X , and small but non-zero abundance of X occurs due to the “freeze-in” annihilation, $\text{SM} \rightarrow X^{++}X^{--}$, suppressed by $\exp(-2m_X/T_{rh})$, or due to the non-thermal inflaton decay, $I \rightarrow \text{SM} + X^{++}X^{--}$. The latter can occur if the mass of the inflaton is larger than $2m_X$. Thus, one can identify two

broad scenarios for the X^{--} abundance:

$$A : \text{Freeze-out, } X^{++}X^{--} \rightarrow \text{SM}; \\ X^{--}/H = \mathcal{O}(10^{-2}) \times m_X/\text{TeV}, \quad (7.1)$$

$$B : \text{Freeze-in, } \text{SM} \rightarrow X^{++}X^{--} \text{ or } I \rightarrow \text{SM} + X^{++}X^{--}; \\ X^{--}/H \text{ model-dependent.} \quad (7.2)$$

In scenario B , the expected abundance of X^{--} is small, but is also very model-dependent.

The strength of the BBN limits derived in our work allows us to make several important inferences about the cosmological/particle physics scenarios related to the mass, lifetime and abundance of X particles.

- X^{--} *within collider reach.* LHC should be able to produce $X^{--} + X^{++}$ pairs of TeV rest mass and below. In the conventional freeze-out scenario A (7.1), the BBN limit (figure 4, lower panel) immediately implies that the lifetime of X^{--} should be shorter than about 100 seconds. Such lifetimes would probably be enough for subsequent extraction of these particles and study of their decay properties, but not enough for their significant accumulations via continuous production. Scenario B (7.2) does not constrain the lifetime of X with $m_X \gtrsim 1 \text{ TeV}$, as T_{rh} can be significantly lower [47].
- X^{--} *with very long lifetimes.* If the lifetime of X^{--} is longer than 10^4 s , its initial abundance has to be less than 10^{-8} , which is incompatible with the freeze out expectations of scenario A . In that case, one would have to invoke either some additional non-annihilation mechanisms for the X^{--} depletion or resort to scenario B with $T_{rh} < 0.05m_X$. If the lifetime of X^{--} is comparable to the age of the Universe, *and* these particles are within reach of $\mathcal{O}(10 \text{ TeV})$ energy colliders, the strong isotopic bound (6.1) will apply, signifying that a “natural occurrence” of X^{--} on Earth will be very rare.
- *Non-collider probes of stable X^{--} .* Most of X^{++} or (${}^8\text{Be}X^{--}$) reaching the Earth will chemically appear as very heavy helium moving with velocities $v/c \sim 10^{-3}$. Since the electron binding in helium is rather strong, it is expected that the target atoms (in the atmosphere, rock or detector) will acquire recoil, and produce ionization. It is debatable whether one could re-purpose old searches for magnetic monopoles, see refs. [1, 46], to look for such signal. At the same time, dark matter and coherent neutrino scattering experiments, designed to detect keV and sub-keV recoils, will be able to pick the collisions of X^{++} or (${}^8\text{Be}X^{--}$) with target atoms. Some of these detectors operate near the Earth’s surface, so that the velocities of X -particles will not be moderated by the overburden (see e.g. [48]). Additional opportunities in this direction are provided by large scintillator-based neutrino telescopes [49].
- *Anomalous isotopes of elements other than He and H.* In addition to (${}^8\text{Be}X^{--}$) and (${}^6\text{Li}X^{--}$), which in the case of stable or practically stable X^{--} should currently appear as abnormal He and H, CBBN predicts that a sizeable fraction of X^{--} will end up bound to ${}^4\text{He}$. Such (${}^4\text{He}X^{--}$) states would appear as abnormally heavy neutrons. When entering the Earth’s atmosphere with CR, they would experience fast exothermic

charge exchange reactions, transferring their X^{--} to nitrogen and oxygen, which would then appear as abnormally heavy boron and carbon, respectively. If $(^4\text{He}X^{--})$ are present at the time of formation of the Earth, they may also transfer their X^{--} to heavier elements, such as e.g. iron and silicon, which would then appear as anomalously heavy chromium and magnesium, respectively. For example, as a result of charge exchange one could have the reaction $(^4\text{He}X^{--}) + ^{14}\text{N} \rightarrow (^{14}\text{N}X^{--}) + ^4\text{He}$ as well as X^{--} release via $(^4\text{He}X^{--}) + ^{14}\text{N} \rightarrow X^{--} + ^{18}\text{F}$. Such reactions should lead to a much higher ionization yield per unit length travelled subsequently by X^{--} . These new anomalously heavy isotopes can also be present in meteorites. Searching for such abnormal isotopes would be of considerable interest.

- X^{--} as dark matter. The BBN bound (5.2) implies that in order for X^{--} to saturate the DM density, its mass has to be close to 10^{10} GeV or above. Most of the DM will then be in the form of $(^8\text{Be}X^{--})$, $(^4\text{He}X^{--})$ and $(X^{++}e^-e^-)$. With such masses, DM will certainly be out of reach of both current and future colliders. While for $m_X \sim 10^4$ GeV or so the bound states of X^{--} with Be, Li, N and O can accumulate at the Earth's surface or in the upper crust and can be searched for there, in the case of $m_X \gtrsim 10^{10}$ GeV they will likely sink to the Earth's core and therefore will not be accessible. In that case, however, their accumulations may still exist in meteorites, where also bound states of X^{--} with Fe and Si can be present. Thus, should the DM consist of the doubly charged X -particles and their bound states, the best strategy for foraging for DM would be to look for anomalous isotopes of known elements in CR and meteorites.

In conclusion, we have derived BBN constraints on abundance vs. lifetime of X^{--} particles through the catalysis of the lithium production. The output of lithium in this CBBN scenario can exceed the standard results by many orders of magnitude. For parametrically long lifetimes, our results imply X^{--}/H to be at or below 10^{-9} level. If the abundance of metastable X^{--} is regulated by the freeze-out processes, which can be considered as the most predictive scenario, then the lifetimes of X^{--} are limited to about 100 seconds.

Acknowledgments

We would like to thank Drs. N. Dalal and K. Olive for useful discussions. M.P. is supported in part by U.S. Department of Energy Grant No. desc0011842. He also acknowledges the hospitality of Perimeter Institute in Canada, where part of this work was carried out. Research at Perimeter Institute is supported by the Government of Canada through the Department of Innovation, Science and Economic Development and by the Province of Ontario through the Ministry of Research and Innovation.

References

- [1] M.L. Perl et al., *The search for stable, massive, elementary particles*, *Int. J. Mod. Phys. A* **16** (2001) 2137 [[hep-ex/0102033](#)] [[INSPIRE](#)].
- [2] ATLAS collaboration, *Search for heavy charged long-lived particles in the ATLAS detector in 36.1 fb^{-1} of proton-proton collision data at $\sqrt{s} = 13$ TeV*, *Phys. Rev. D* **99** (2019) 092007 [[arXiv:1902.01636](#)] [[INSPIRE](#)].

- [3] CMS collaboration, *Search for long-lived charged particles in proton-proton collisions at $\sqrt{s} = 13$ TeV*, *Phys. Rev. D* **94** (2016) 112004 [[arXiv:1609.08382](https://arxiv.org/abs/1609.08382)] [[INSPIRE](https://inspirehep.net/search?p=find+EPRINT+arXiv:1609.08382)].
- [4] W.H. Breunlich, P. Kammler, J.S. Cohen and M. Leon, *Muon-catalyzed fusion*, *Ann. Rev. Nucl. Part. Sci.* **39** (1989) 311 [[INSPIRE](https://inspirehep.net/search?p=find+J+Ann. Rev. Nucl. Part. Sci.+39+1989+311)].
- [5] K. Hamaguchi, T. Hatsuda, M. Kamimura and T.T. Yanagida, *Stau-catalyzed d-t nuclear fusion*, [arXiv:1202.2669](https://arxiv.org/abs/1202.2669) [[INSPIRE](https://inspirehep.net/search?p=find+EPRINT+arXiv:1202.2669)].
- [6] E. Akhmedov, *Nuclear fusion catalyzed by doubly charged scalars: implications for energy production*, *Phys. Rev. D* **106** (2022) 035013 [[arXiv:2109.13960](https://arxiv.org/abs/2109.13960)] [[INSPIRE](https://inspirehep.net/search?p=find+EPRINT+arXiv:2109.13960)].
- [7] ATLAS collaboration, *Search for heavy, long-lived, charged particles with large ionisation energy loss in pp collisions at $\sqrt{s} = 13$ TeV using the ATLAS experiment and the full run 2 dataset*, *JHEP* **06** (2023) 158 [[arXiv:2205.06013](https://arxiv.org/abs/2205.06013)] [[INSPIRE](https://inspirehep.net/search?p=find+EPRINT+arXiv:2205.06013)].
- [8] ATLAS collaboration, *Exploration at the high-energy frontier: ATLAS run 2 searches investigating the exotic jungle beyond the Standard Model*, [arXiv:2403.09292](https://arxiv.org/abs/2403.09292) [[INSPIRE](https://inspirehep.net/search?p=find+EPRINT+arXiv:2403.09292)].
- [9] G.F. Giudice, M. McCullough and D. Teresi, *dE/dx from boosted long-lived particles*, *JHEP* **08** (2022) 012 [[arXiv:2205.04473](https://arxiv.org/abs/2205.04473)] [[INSPIRE](https://inspirehep.net/search?p=find+EPRINT+arXiv:2205.04473)].
- [10] E. Akhmedov, P.S.B. Dev, S. Jana and R.N. Mohapatra, *Long-lived doubly charged scalars in the left-right symmetric model: catalyzed nuclear fusion and collider implications*, *Phys. Lett. B* **852** (2024) 138616 [[arXiv:2401.15145](https://arxiv.org/abs/2401.15145)] [[INSPIRE](https://inspirehep.net/search?p=find+EPRINT+arXiv:2401.15145)].
- [11] M. Pospelov, *Particle physics catalysis of thermal Big Bang nucleosynthesis*, *Phys. Rev. Lett.* **98** (2007) 231301 [[hep-ph/0605215](https://arxiv.org/abs/hep-ph/0605215)] [[INSPIRE](https://inspirehep.net/search?p=find+EPRINT+hep-ph/0605215)].
- [12] PARTICLE DATA GROUP collaboration, *Review of particle physics*, *PTEP* **2022** (2022) 083C01 [[INSPIRE](https://inspirehep.net/search?p=find+J+PTEP+2022+083C01)].
- [13] D. Fargion, M. Khlopov and C.A. Stephan, *Cold dark matter by heavy double charged leptons?*, *Class. Quant. Grav.* **23** (2006) 7305 [[astro-ph/0511789](https://arxiv.org/abs/astro-ph/0511789)] [[INSPIRE](https://inspirehep.net/search?p=find+EPRINT+astro-ph/0511789)].
- [14] J.-R. Cudell, M. Khlopov and Q. Wallemacq, *Some potential problems of OHe composite dark matter*, *Bled Workshops Phys.* **15** (2014) 66 [[arXiv:1412.6030](https://arxiv.org/abs/1412.6030)] [[INSPIRE](https://inspirehep.net/search?p=find+EPRINT+arXiv:1412.6030)].
- [15] P. Mueller et al., *Search for anomalously heavy isotopes of helium in the earth's atmosphere*, *Phys. Rev. Lett.* **92** (2004) 022501 [[nucl-ex/0302025](https://arxiv.org/abs/nucl-ex/0302025)] [[INSPIRE](https://inspirehep.net/search?p=find+EPRINT+nucl-ex/0302025)].
- [16] P.F. Smith et al., *A search for anomalous hydrogen in enriched D_2O , using a time-of-flight spectrometer*, *Nucl. Phys. B* **206** (1982) 333 [[INSPIRE](https://inspirehep.net/search?p=find+J+Nucl. Phys. B+206+1982+333)].
- [17] P. Verkerk et al., *Search for superheavy hydrogen in sea water*, *Phys. Rev. Lett.* **68** (1992) 1116 [[INSPIRE](https://inspirehep.net/search?p=find+J+Phys. Rev. Lett.+68+1992+1116)].
- [18] R.N. Mohapatra and G. Senjanovic, *Neutrino mass and spontaneous parity nonconservation*, *Phys. Rev. Lett.* **44** (1980) 912 [[INSPIRE](https://inspirehep.net/search?p=find+J+Phys. Rev. Lett.+44+1980+912)].
- [19] T.-H. Yeh, K.A. Olive and B.D. Fields, *The impact of new $d(p, \gamma)^3He$ rates on big bang nucleosynthesis*, *JCAP* **03** (2021) 046 [[arXiv:2011.13874](https://arxiv.org/abs/2011.13874)] [[INSPIRE](https://inspirehep.net/search?p=find+EPRINT+arXiv:2011.13874)].
- [20] R. Consiglio et al., *PArthENoPE reloaded*, *Comput. Phys. Commun.* **233** (2018) 237 [[arXiv:1712.04378](https://arxiv.org/abs/1712.04378)] [[INSPIRE](https://inspirehep.net/search?p=find+EPRINT+arXiv:1712.04378)].
- [21] C. Pitrou, A. Coc, J.-P. Uzan and E. Vangioni, *A new tension in the cosmological model from primordial deuterium?*, *Mon. Not. Roy. Astron. Soc.* **502** (2021) 2474 [[arXiv:2011.11320](https://arxiv.org/abs/2011.11320)] [[INSPIRE](https://inspirehep.net/search?p=find+EPRINT+arXiv:2011.11320)].

[22] M. Asplund et al., *Lithium isotopic abundances in metal-poor halo stars*, *Astrophys. J.* **644** (2006) 229 [[astro-ph/0510636](#)] [[INSPIRE](#)].

[23] T.P. Walker et al., *Primordial nucleosynthesis redux*, *Astrophys. J.* **376** (1991) 51 [[INSPIRE](#)].

[24] F. Spite and M. Spite, *Abundance of lithium in unevolved halo stars and old disk stars: interpretation and consequences*, *Astron. Astrophys.* **115** (1982) 357 [[INSPIRE](#)].

[25] B.D. Fields and K.A. Olive, *Implications of the non-observation of ${}^6\text{Li}$ in halo stars for the primordial ${}^7\text{Li}$ problem*, *JCAP* **10** (2022) 078 [[arXiv:2204.03167](#)] [[INSPIRE](#)].

[26] R.H. Cyburt, B.D. Fields and K.A. Olive, *An update on the big bang nucleosynthesis prediction for ${}^7\text{Li}$: the problem worsens*, *JCAP* **11** (2008) 012 [[arXiv:0808.2818](#)] [[INSPIRE](#)].

[27] K. Jedamzik and M. Pospelov, *Big bang nucleosynthesis and particle dark matter*, *New J. Phys.* **11** (2009) 105028 [[arXiv:0906.2087](#)] [[INSPIRE](#)].

[28] M. Pospelov and J. Pradler, *Big bang nucleosynthesis as a probe of new physics*, *Ann. Rev. Nucl. Part. Sci.* **60** (2010) 539 [[arXiv:1011.1054](#)] [[INSPIRE](#)].

[29] B.D. Fields, *The primordial lithium problem*, *Ann. Rev. Nucl. Part. Sci.* **61** (2011) 47 [[arXiv:1203.3551](#)] [[INSPIRE](#)].

[30] S. Kawanomoto, K.T. Suzuki, H. Ando and T. Kajino, *First detection of ${}^7\text{Li}/{}^6\text{Li}$ -ratio in the interstellar medium beyond the solar-system, and its impact on primordial ${}^7\text{Li}$* , *Nucl. Phys. A* **718** (2003) 659 [[INSPIRE](#)].

[31] D.C. Knauth, S.R. Federman and D.L. Lambert, *An ultra-high-resolution survey of the interstellar ${}^7\text{Li}$ -to- ${}^6\text{Li}$ isotope ratio in the solar neighborhood*, *Astrophys. J.* **586** (2003) 268 [*Erratum ibid.* **594** (2003) 664] [[astro-ph/0212233](#)] [[INSPIRE](#)].

[32] T. Prodanovic and B.D. Fields, *Probing primordial and pre-galactic lithium with high velocity clouds*, *Astrophys. J. Lett.* **616** (2004) L115 [[astro-ph/0412238](#)] [[INSPIRE](#)].

[33] S. Kawanomoto et al., *The new detections of ${}^7\text{Li}/{}^6\text{Li}$ isotopic ratio in the interstellar media*, *Astrophys. J.* **701** (2009) 1506.

[34] J.C. Howk, N. Lehner, B.D. Fields and G.J. Mathews, *The detection of interstellar lithium in a low-metallicity galaxy*, *Nature* **489** (2012) 121 [[arXiv:1207.3081](#)] [[INSPIRE](#)].

[35] E. Anders and N. Grevesse, *Abundances of the elements: meteoritic and solar*, *Geochim. Cosmochim. Acta* **53** (1989) 197 [[INSPIRE](#)].

[36] J. Geiss and G. Gloeckler, *Abundances of deuterium and helium-3 in the protosolar cloud*, *Space Sci. Rev.* **84** (1998) 239.

[37] S.D. Friedman et al., *A high-precision survey of the D/H ratio in the nearby interstellar medium*, *Astrophys. J.* **946** (2023) 34 [[arXiv:2301.13226](#)].

[38] H. An, M. Pospelov and J. Pradler, *Direct constraints on charged excitations of dark matter*, *Phys. Rev. Lett.* **109** (2012) 251302 [[arXiv:1209.6358](#)] [[INSPIRE](#)].

[39] A. Berlin, H. Liu, M. Pospelov and H. Raman, *Low-energy signals from the formation of dark-matter-nucleus bound states*, *Phys. Rev. D* **105** (2022) 095028 [[arXiv:2110.06217](#)] [[INSPIRE](#)].

[40] I. Angeli and K.P. Marinova, *Table of experimental nuclear ground state charge radii: an update*, *Atom. Data Nucl. Data Tabl.* **99** (2013) 69 [[INSPIRE](#)].

[41] M. Pospelov, *Bridging the primordial $A=8$ divide with catalyzed big bang nucleosynthesis*, [arXiv:0712.0647](#) [[INSPIRE](#)].

- [42] M. Pospelov, J. Pradler and F.D. Steffen, *Constraints on supersymmetric models from catalytic primordial nucleosynthesis of beryllium*, *JCAP* **11** (2008) 020 [[arXiv:0807.4287](https://arxiv.org/abs/0807.4287)] [[INSPIRE](#)].
- [43] M. Kamimura, Y. Kino and E. Hiyama, *Big-bang nucleosynthesis reactions catalyzed by a long-lived negatively-charged leptonic particle*, *Prog. Theor. Phys.* **121** (2009) 1059 [[arXiv:0809.4772](https://arxiv.org/abs/0809.4772)] [[INSPIRE](#)].
- [44] G.R. Caughlan and W.A. Fowler, *Thermonuclear reaction rates. 5*, *Atom. Data Nucl. Data Tabl.* **40** (1988) 283 [[INSPIRE](#)].
- [45] G.G. Ryzhikh, R.A. Eramzhyan and S. Shlomo, $\alpha - d$ capture with formation of ${}^6\text{Li}$ and the isoscalar $E1$ multipole, *Phys. Rev. C* **51** (1995) 3240 [Erratum *ibid.* **53** (1996) 2560] [[INSPIRE](#)].
- [46] S. Burdin et al., *Non-collider searches for stable massive particles*, *Phys. Rept.* **582** (2015) 1 [[arXiv:1410.1374](https://arxiv.org/abs/1410.1374)] [[INSPIRE](#)].
- [47] A. Kudo and M. Yamaguchi, *Inflation with low reheat temperature and cosmological constraint on stable charged massive particles*, *Phys. Lett. B* **516** (2001) 151 [[hep-ph/0103272](https://arxiv.org/abs/hep-ph/0103272)] [[INSPIRE](#)].
- [48] CONUS collaboration, *Constraints on elastic neutrino nucleus scattering in the fully coherent regime from the CONUS experiment*, *Phys. Rev. Lett.* **126** (2021) 041804 [[arXiv:2011.00210](https://arxiv.org/abs/2011.00210)] [[INSPIRE](#)].
- [49] J. Bramante et al., *Foraging for dark matter in large volume liquid scintillator neutrino detectors with multiscatter events*, *Phys. Rev. D* **99** (2019) 083010 [[arXiv:1812.09325](https://arxiv.org/abs/1812.09325)] [[INSPIRE](#)].